



Removal of Malachite Green Dye from Aqueous Solutions onto Microwave Assisted Zinc Chloride Chemical Activated Epicarp of *Ricinus communis*

M. Makeswari, T. Santhi*

Department of Chemistry, Karpagam University, Coimbatore, India

Email: *ssnilasri@yahoo.co.in

Received October 4, 2012; revised November 20, 2012; accepted January 15, 2013

ABSTRACT

Competitive adsorption of malachite green (MG) in single and binary system on microwave activated epicarp of *Ricinus communis* (MRC) and microwave assisted zinc chloride activated epicarp of *Ricinus communis* (ZRC) were analyzed. The preparation of ZRC from *Ricinus communis* was investigated in this paper. Orthogonal array experimental design method was used to optimize the preparation of ZRC. Optimized parameters were radiation power of 100 W, radiation time of 4 min, concentration of zinc chloride of 30% by volume and impregnation time of 16 h, respectively. The MRC and ZRC were characterized by pHzpc, SEM-EDAX and FTIR analysis. The effect of the presence of one dye solution on the adsorption of the other dye solution was investigated in terms of equilibrium isotherm and adsorption yield. Experimental results indicated that the uptake capacities of one dye were reduced by the presence of the other dye. The adsorption equilibrium data fits the Langmuir model well and follows pseudo second-order kinetics for the bio-sorption process. Among MRC and ZRC, ZRC shows most adsorption ability than MRC in single and binary system.

Keywords: Epicarp of *Ricinus communis*; Microwave Heating; Zinc Chloride; Binary System; Equilibrium Isotherm

1. Introduction

Dyes are widely used in industries such as textiles, leather, paper, plastics, etc. to color their final products. The textile industries are the greatest generators of liquid effluent, due to high quantity of water used in the dyeing processes [1]. Fifteen percent of the total world production of dyes is lost during the dyeing process and is released in textile effluent. Malachite Green (MG) is a cationic dye and widely used for the dyeing of leather, wool and silk, distilleries, jute, paper, as a food coloring agent, food additive, in medical disinfectant and fish industries [2,3]. Discharge of MG into the hydrosphere can cause environmental degradation as it gives undesirable color to water and reduces sunlight penetration. The consumption of MG has many adverse effects due to its carcinogenic, genotoxic, mutagenic and teratogenic properties of MG are due to presence of the nitrogen.

Dye removal from wastewater effluent is a major environmental problem because of the difficulty of treating such streams by conventional physical, chemical, physico-chemical and biological treatment methods. Many physical and chemical treatment methods including adsorption, coagulation, precipitation filtration, electrodi-

alysis, membrane separation and oxidation have been used for the treatment of dye-containing effluents [4]. Adsorption process is one of the most effective and economically feasible methods for the removal of dyes from aqueous solutions.

Activated carbon was widely used in removal dyes from textile effluent, which had relatively high sorption capacity for a wide variety of dyes. Commercially available activated carbons are usually derived from natural materials such as wood or coal, therefore, are still considered expensive [5]. Due to economical reasons, it was investigated for a long time that agricultural byproducts and waste materials used for the production of activated carbon. Examples of these attempts included rattan sawdust [6], rice husk [7], lemon peel [8], granular kohlrabi [9], jute fiber [10] and coconut husk [11].

Two methods are used for the preparation of AC via, physical and chemical activation. During physical activation, the raw material is carbonized first at high temperature and then it is activated by CO₂ or steam under pressure to increase porosity and surface area of AC. In chemical activation both carbonization and activation takes place simultaneously, in which raw material is first impregnated with activating chemical and then carbonized at desired temperature that varies according to acti-

*Corresponding author.

vating chemical used [12]. The development of porous structure is better in the case of chemical activation [13]. Chemical activation is held in presence of dehydrating reagents such as KOH, K_2CO_3 , NaOH, $ZnCl_2$ and H_3PO_4 which influence pyrolytic decomposition and inhibit tar formation. The carbon yield obtained is higher and the temperature used in chemical activation is lower than that of physical activation. Behaviors of the reagents during chemical activation show different effects on the final product. $ZnCl_2$ is the widely used as activating reagent, since it resulted in high surface areas and high yield [14,15]. In the use of $ZnCl_2$, the activated carbons had large surface areas and more micro pore structure [8, 10]. For preparing activated carbon, conventional heating method is usually adopted, in which the energy is produced by electrical furnace. Recently, microwave heating technology has been applied to fabricate activated carbon due to its rapid heating and uniformity [15].

The application of microwave (MW) heating technology for regenerating industrial waste activated carbon has been investigated with very promising results [16, 17]. The main difference between MW devices and conventional heating systems is in the way of t heating. In the MW device, the microwaves supply energy directly to the carbon bed. Energy transfer is not by conduction or convection as in conventional heating, but microwave energy is readily transformed heat into inside the particles by dipole rotation and ionic conduction [16-18]. Recently microwave energy has been widely using in several fields of applications on both research and industrial processes. Although the use of microwave energy changes the properties of carbonaceous materials very much, there are relatively few publications that describe the use of microwaves for producing and regenerating activated carbons. Nabasis *et al.*, studied on the surface chemistry modification of activated carbon fibres by means of microwave heating which was found to be very effective. Microwave is now being used in various fields in order to heat dielectric materials because it can considerably shorten the treatment time and reduce energy consumption.

The aim of the present work was to optimize the MRC and ZRC preparation conditions using orthogonal array experimental design method, investigate the ability of a malachite green dye sorbent prepared from epicarp of *Ricinus communis* (RC) is an agricultural waste material by microwave assisted chemical activation using zinc chloride as activating agent for the adsorption of malachite green dye from aqueous solution. The adsorption ability of classical activated *Ricinus communis* was previously investigated for the adsorption of MG dye from aqueous solution [19].

The objective of the present study is to evaluate the possibility of using the dried epicarp of *Ricinus commu-*

nis to develop a new low-cost activated carbon and to study the effect of several parameters (pH, contact time, initial metal concentration, pH_{zpc} , adsorption isotherms and kinetics) on the adsorption efficiency of malachite green (MG) dye from aqueous solution in single and binary system and compare the performance of MRC and ZRC for the adsorption of MG in single (MG) and binary system (MG + Methylene blue).

2. Experimental

2.1. Materials

Samples of Malachite green (MG) and Methylene blue (MB) were obtained from Aluva, Edayar (specrum reagents and chemicals pvt. Ltd). All other chemicals used in this study were analytical grade and Purchased from Aluva, Edayar (specrum reagents and chemicals pvt. Ltd) and was used without any further purification. The chemical structure of malachite green is shown in **Figure 1**. Malachite green hydrochloride (C.I. = 42,000) has the molecular formula of $C_{23}H_{25}ClN_2$, the molecular weight of 364.92, $\lambda_{max} = 617$ nm.

A Stock solution of 500 mg/L was prepared by dissolving accurately weighed amounts of MG in doses of 1000 mL distilled water. The desirable experimental concentrations of solutions were prepared by diluting the stock solution with distilled water when necessary.

2.2. Preparation of Adsorbent

2.2.1. Preparation of Microwave Treated *Ricinus communis* (MRC)

The epicarp of *Ricinus communis* (RC) was obtained from an agricultural form in Tirupur district (TamilNadu). It was air-dried and powdered in a grinder. Dried *Ricinus communis* with the mass of 6 g were placed in a MW heating apparatus (MW71E) which produced by SAMSUNG, Malaysia. After a certain heating power of 100 W and microwave radiation time of 4 min, and finally dried at $150^\circ C$ in a hot air oven. The MRC was then stored in an air-tight container for later experimental use.

2.2.2. Preparation of Zinc Chloride Assisted *Ricinus communis* (ZRC)

The epicarp of *Ricinus communis* was obtained from the

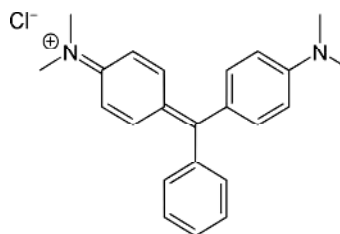


Figure 1. Chemical structure of malachite green.

agricultural form in Tirupur district (Tamil Nadu). It was air-dried and powdered in a grinder. Dried *Ricinus communis* with the mass of 6 g were mixed with 30 mL of ZnCl₂ to vary concentrations in the range of 30% - 60% by volume. The slurry was kept at room temperature for various time spans in the range of 16 - 28 h to ensure the access of the ZnCl₂ to the *Ricinus communis*. After mixing, the slurry was placed in a MW heating apparatus (MW71E, SAMSUNG). After a heating power of 100 W - 600 W and microwave radiation time of 10 min - 4 min, the carbonized sample were washed with 0.5 M HCl, hot water and cold distilled water until the pH of the washing solution reached 6 - 7, filtered and finally dried at 150°C in hot air oven for 6 h. The ZRC was then stored in an air-tight container for later experimental use.

2.3. Optimization of ZRC Preparation Conditions

In order to optimize the preparation conditions of the ZRC, Taguchi experimental design method was used [19]. An L₁₆ orthogonal array with four operational parameters each in four levels was used to evaluate the corresponding optimal values. These variables and their values are summarized in **Table 1**. The complete design matrix of the experiments and the obtained results are shown in **Table 2**. Iodine is considered as probe molecules for assessing the adsorption capacity of adsorbents for solutes of molecular sizes less than 10 Å. Iodine number was normally listed as specification parameter for ZRC. Therefore, the responses were iodine number (Y₂, mg/g), yield (Y₁, %) was obtained at 25°C ± 1°C on the basis of the standard Test method. The yield of the carbon samples was estimated according to,

$$Y = \frac{M}{M_0} \times 100 \quad (1)$$

where M is the weight of MRC and ZRC and M₀ is the weight of air dried *Ricinus communis* leaves.

2.4. Effect of Independent Variables on ZRC Preparation Conditions

According to the L₁₆ array designed by Taguchi method,

Table 1. Design and levels.

Independent variables	Symbol	Range and levels			
		1	2	3	4
Radiation power (W)	A	100	200	400	600
Radiation time (min)	B	10	8	6	4
Concentration of ZnCl ₂ (vol%)	C	30	40	50	60
Impregnation time (h)	D	16	20	24	28

Table 2. Experimental design matrix and results.

Runs	Variables				Responses (Y)	
	A	B	C	D	Iodine number (y ₁ , mg/g)	Yield of ZRC (y ₂ , %)
1	1	1	1	1	466.0	35.74
2	2	1	1	1	698.56	54.88
3	3	1	1	1	910.16	72.21
4	4	1	1	1	783.16	69.68
5	1	1	1	1	635.0	43.98
6	1	2	1	1	973.66	53.32
7	1	3	1	1	1164.6	58.75
8	1	4	1	1	466.00	35.74
9	1	1	1	1	466.0	35.74
10	1	1	2	1	762.33	52.62
11	1	1	3	1	804.33	63.11
12	1	1	4	1	719.66	56.94
13	1	1	1	1	466.0	35.74
14	1	1	1	2	740.83	42.16
15	1	1	1	3	402.16	52.95
16	1	1	1	4	825.5	55.97

16 different ZRC samples were prepared. Iodine number and yield of each sample were determined and shown in **Table 2**. The effect of operational parameters on responses of the prepared ZRC samples is shown in **Figure 2**.

2.4.1. Effect of Microwave Radiation Power on the Yield and Iodine Number of ZRC

Effect of microwave radiation power (Parameter A) on adsorption capacity and the yield of ZRC were evaluated under the concentration of ZnCl₂ (X_{Zn}) of 30 ml and microwave radiation time of 4 min. **Figure 2** shows that the yield of ZRC samples were increased with the increasing of microwave power level from 100 - 400 W, and then decreased with increasing of the level of 600 W. There were similar tendency of the iodine number on ZRC. The possible reason was that the higher energy was offered to the samples with increasing the power level, the more active sites and pores on the samples. When microwave power reached a certain level, overfull energy could make a small quantity of carbon burnt, and the structure of pores was destroyed. Similar results have been obtained by other researchers [9,21].

2.4.2. Effect of Microwave Radiation Time on the Yield and Iodine Number of ZRC

Effects of microwave radiation time (parameter B) on the

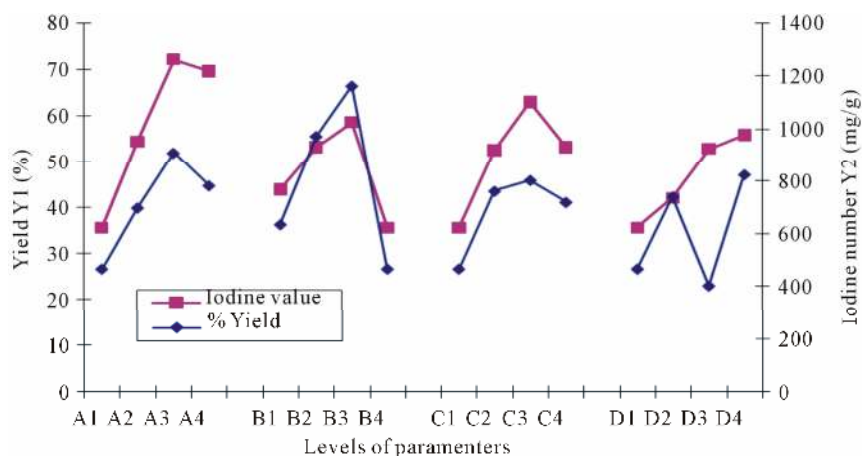


Figure 2. The effect of operational parameters on responses of the prepared ZRC samples. ((A) Radiation power; (B) Radiation time; (C) Concentration of $ZnCl_2$ and (D) Impregnation time).

yield and iodine number of ZRC were evaluated, under the conditions of X_{Zn} of 30 ml and microwave power of 100 W (Figure 2). It revealed that the yield of ZRC was increased with increasing the radiation time up to 8 min, and then decreased, when the time was increased to 10 min. There were same tendency of the iodine number of ZRC. Similar trends were also found by Li *et al.*, when they prepared the activated carbon from tobacco stems using microwave radiation [22]. The activation degree was much more dependent on the microwave radiation time. With the prolongation of microwave radiation time, much more active sites and pores were formed on the surface of samples. Therefore the adsorption capacity of ZRC would be increased with the prolongation of microwave radiation time. However, when microwave radiation time reached a certain value, the pores of carbon would be burnt off by microwave heating, which would lower the iodine number, the amount of nickel uptake and the yield of ZRC.

2.4.3. Effect of Impregnation Ratio of $ZnCl_2$ and Impregnation Time on the Yield and Iodine Number of ZRC

Under the microwave power of 100 W, radiation time of 8 min, the effects of the impregnation ratio (parameter C) of $ZnCl_2$ on the yield and iodine number of ZRC was studied (Figure 2). With the increasing X_{Zn} from 30 ml to 90 ml, the yield, the iodine number and the amount of MG adsorption of ZRC were all increased. While X_{Zn} was further increased to 120 ml, these two parameters were all decreased. With increase in impregnation ratio, the initial effect of $ZnCl_2$ is to inhibit the release of volatile matter, which results in higher yield and iodine number of ZRC. Subsequently, with the further increase in impregnation ratio, the zinc chloride assumed a dehydration agent role during activation. It inhibits the formation of tars and any other liquids that could clog up the

pores of the sample, the movement of the volatiles through the pore passages would not be hindered, the volatiles will be subsequently released from the carbon surface during activation. Therefore the yield and iodine number of carbon were all decreased. Similar trends were also reported by Lua and Yang [23], Guo and Lua [24] in their studies on the preparation of activated carbon from pistachio-nut shell and oil-palm shells, respectively.

The results presented in Figure 2 also shows that impregnation time (parameter D) had little influence on the yield and iodine number. The action of $ZnCl_2$ on the lignocellulosic material could be expressed as the following mechanism.

During impregnation stage the base attacked the cellular structure of *Ricinus communis* leaves, forming cleavage to the linkages between the lignin and cellulose. It was followed by recombination reactions, where larger structural units and strong cross linked solids were formed. This base worked, principally, in early stage during impregnation and might extended to have a slight effect in the carbonization stage [25].

2.5. Optimized Conditions

In the production of AC, relatively high product yield and adsorption capacity were expected. Therefore, more attention should be paid to improve the carbon yield and enhance its adsorption capacity for economical viability. However, it was difficult to optimize both these responses under the same condition, for the different interest in different region. From the discussions mentioned above, the microwave radiation power, microwave radiation time, impregnation ratio and the impregnation time of $ZnCl_2$ had significant effects on the yield and the adsorption capacity of the activated carbon from *Ricinus communis* leaves with $ZnCl_2$ activation by microwave radiation. Therefore the optimum conditions were ob-

tained as following: the microwave power of 100 W, microwave radiation time of 4 min, X_{Zn} of 30 ml and impregnation time of 16 h. Iodine number and the yield of activated carbon prepared under optimum conditions were 69.68% and 783.16 (mg/g), respectively. The ZRC was used in the characterization analysis and adsorption experiments which were prepared under optimum conditions.

2.6. Characterization of MRC and ZRC

The surface morphology of MRC and ZRC were identified by using SEM technique (Jeol jsm-6390). A Fourier transforms infrared spectroscopy (SHIMADZU, IR Affinity-1) with KBr pellet was used to study surface functional groups of the MRC and ZRC, with a scanning range of 4000 - 400 cm^{-1} . The zero surface charges (pH_{ZPC}) of MRC and ZRC were determined by using the solid addition method [20]. The acidity and Basicity of MRC and ZRC were determined and confirmed by Boehm's titration method. The ability of the MRC and ZRC in the adsorption of MG in single (MG) and binary system (MG + MB) were investigated by batch isotherm and kinetic studies. The concentration of MG in single and binary system were determined using a double beam UV-vis spectrophotometer (SHIMADZU UV-2450) of the wavelength of 617 nm.

2.7. Batch Equilibrium Studies

To study the effect of parameters such as adsorbent dose, dye concentration and solution pH for the removal of adsorbate on MRC and ZRC, batch experiments were performed. Stock solutions of MG in single and binary system were prepared by dissolving MG (S) and MG + MB (B) in deionized water and further diluted to the 50 - 200 mg/L concentrations for the experiments. pH was adjusted by adding 0.1 M HCl or 0.1 M NaOH into the solutions with known initial MG concentrations. Batch adsorption experiments were conducted in asset of 250 mL stoppered flasks containing 0.2 g of MRC and ZRC and 50 mL of dye solutions with different concentrations (50, 100, 150 and 200 mg/L) at pH 5. The flasks were agitated using a mechanical orbital shaker, and maintained at room temperature for 2 h until the equilibrium was reached. The suspensions were filtered and dye concentrations in the supernatant solutions were measured using a UV-vis spectrophotometer at 617 nm. The amounts of uptake of MG by MRC and ZRC in the equilibrium (q_e) were calculated by the following mass-balance relationship

$$q_e = \frac{(C_o - C_e)}{W} \times V \quad (2)$$

where C_o and C_e (mg/L) are the liquid phase concentra-

tions of dye at initial and equilibrium, respectively. V (L) is the volume of the solution, and W (g) is the mass of adsorbent used.

Adsorption isotherm is the most important information which indicates how the adsorbate molecules distribute between the liquid phase and the solid phase when adsorption process reaches on equilibrium state. When the system is at equilibrium is of importance in determining the maximum sorption capacity of MRC and ZRC towards dyes.

2.7.1. Effect of Adsorbent Dose

To observe the effect of adsorbent dose on dye adsorption, different amounts of adsorbent varying from 0.2 g/50 ml, 0.4 g/50 ml, 0.6 g/50 ml, 0.8 g/50 ml and 1 g/50 ml were added into initial concentration of 100 mg/L MG in single and binary solution. The mixtures were shaken in 250 mL stoppered flasks at room temperature at pH 5 until the equilibrium time was reached.

2.7.2. Effect of Solution pH

To study the effect of solution pH on MG adsorption, 100 mg/L initial concentration at different pH values (2 - 9) was agitated with 0.2 g of MRC and ZRC in a mechanical orbital shaker at room temperature. The effect of pH on MG adsorption was studied by varying the pH from 2.0 to 9.0. The concentration of MG solution used for this study was 100 mg/L and the adsorbent dose was 0.2 g. The initial pH was written as pH_i and the solution pH after adsorption was also measured and written as pH_f . The pH was adjusted with 0.1 M NaOH and 0.1 M HCl solutions.

2.7.3. Effect of Initial Dye Concentration

In order to study the effect of initial dye concentration on the adsorption uptake, MG solutions with initial concentrations of 50 - 200 mg/L with varying the adsorbent dose of 0.2 g/50 mL of MRC and ZRC respectively. In this case, the solution pH was kept as 5.

3. Results and Discussion

3.1. Surface Acidity and Basicity

Surface acidity was estimated by mixing 0.2 g of MRC and ZRC with 25 mL of 0.5 M NaOH in a closed flask, the flask was agitated for 48 h at room temperature (28°C). The Suspension was decanted and the remaining NaOH was titrated with 0.5 M HCl. The surface basicity was measured by titration with 0.5 M NaOH after agitation of 0.2 g of MRC and ZRC with 0.5 M HCl. MRC has the surface acidity of 1.803 mmol/g and 4.06 mmol/g surface basicity and ZRC has the surface acidity of 2.73 mmol/g and 2.53 mmol/g surface basicity. Acidity and basicity were confirmed by Boehm titration method.

Boehm titrations quantify the basic and oxygenated acidic surface groups on activated carbons [21].

3.2. Zero Surface Charges—The Characteristic Analysis of MRC and ZRC

The influence on the solution pH on the dye uptake can be explained on the basis of the pH zero point charge or isoelectric point of the adsorbent. The value of the pH necessary to affect a net zero charge on a solid surface in the absence of specific sorption is called the point of zero charge, pH_{ZPC} .

The zero surface charge of MRC and ZRC were determined by using the solid addition method [20]. The experiment was conducted in a series of 250 mL glass stoppered flasks. Each flask was filled with 50 mL of different initial pH $NaNO_3$ solutions and 0.2 g of MRC and ZRC. The pH values of the $NaNO_3$ solutions were adjusted between 2 to 9 by adding either 0.1 M HNO_3 or 0.1 M $NaOH$. The suspensions were then sealed and shaken for 2 h at 150 rpm. The final pH values of the supernatant liquid were noted. The difference between the initial pH (pH_0) and final pH (pH_f) values ($pH = pH_0 - pH_f$) was plotted against the values of pH_0 . The point of intersection of the resulting curve with abscissa, gave the pH_{ZPC} .

Figures 3(a) and **(b)** shows that the plot between ΔpH , *i.e.* ($pH_0 - pH_f$) and pH_0 for pH_{ZPC} measurement for MRC and ZRC. The point of zero charge for MRC is found to be 3.14 and for ZRC is 4. This result indicated that the pH_{ZPC} of MRC and ZRC were depended on the raw material and the activated carbon. The zero point charge (pH_{ZPC} 3.14 for MRC and pH_{ZPC} 4 for ZRC) is below the solution pH (pH 5) and hence the negative charge density on the surface of MRC and ZRC increased which favours the adsorption of cationic dye [22].

3.3. Functional Group Analysis of MRC and ZRC

The aim of using FTIR analysis is to determine the existence of functional groups and identification of characteristic peaks is based on the studies reported in the literature [23-25]. The FTIR spectrum of MRC and ZRC were shown in **Figures 4(a)** and **(b)**. The absorption bands identify in the spectra and it revealed corresponding functional groups.

The broad band at about 3406.29 cm^{-1} was observed, which was assigned to the O-H stretching vibration of the hydroxyl functional groups including hydrogen bonding. The intense bent at about 2927.94 cm^{-1} for the precursor was attributed to the C-H stretching vibration. The peak at 1639.49 cm^{-1} was characteristics of the C=O stretching vibration of lactonic and carbonyl groups. The peaks occurring at 1396.46 cm^{-1} , 1185.00 cm^{-1} were all as-

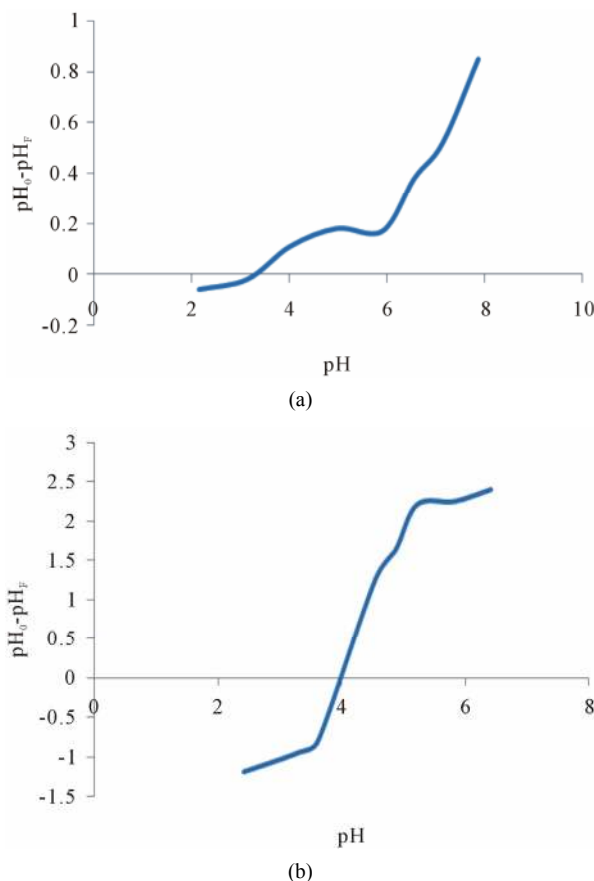


Figure 3. Zero point charges of (a) MRC and (b) ZRC.

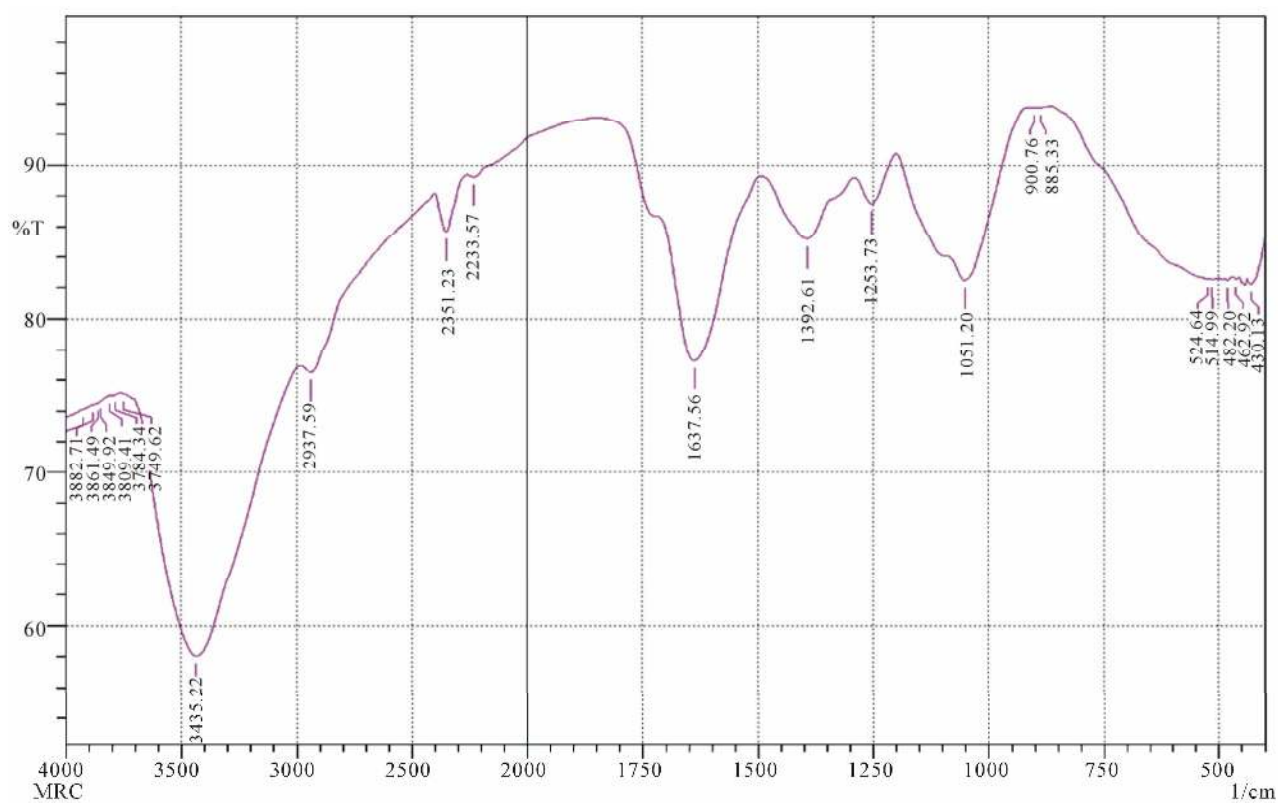
cribed to oxygen functionalities such as highly conjugated C-O stretching, C-O stretching in carboxylic groups, and carboxylate moieties. The band located at 2352.6 cm^{-1} and 2332.6 cm^{-1} are attributed to the C≡C stretching is due to the $ZnCl_2$ activation [26].

3.4. Scanning Electron Microscopic (SEM) Studies

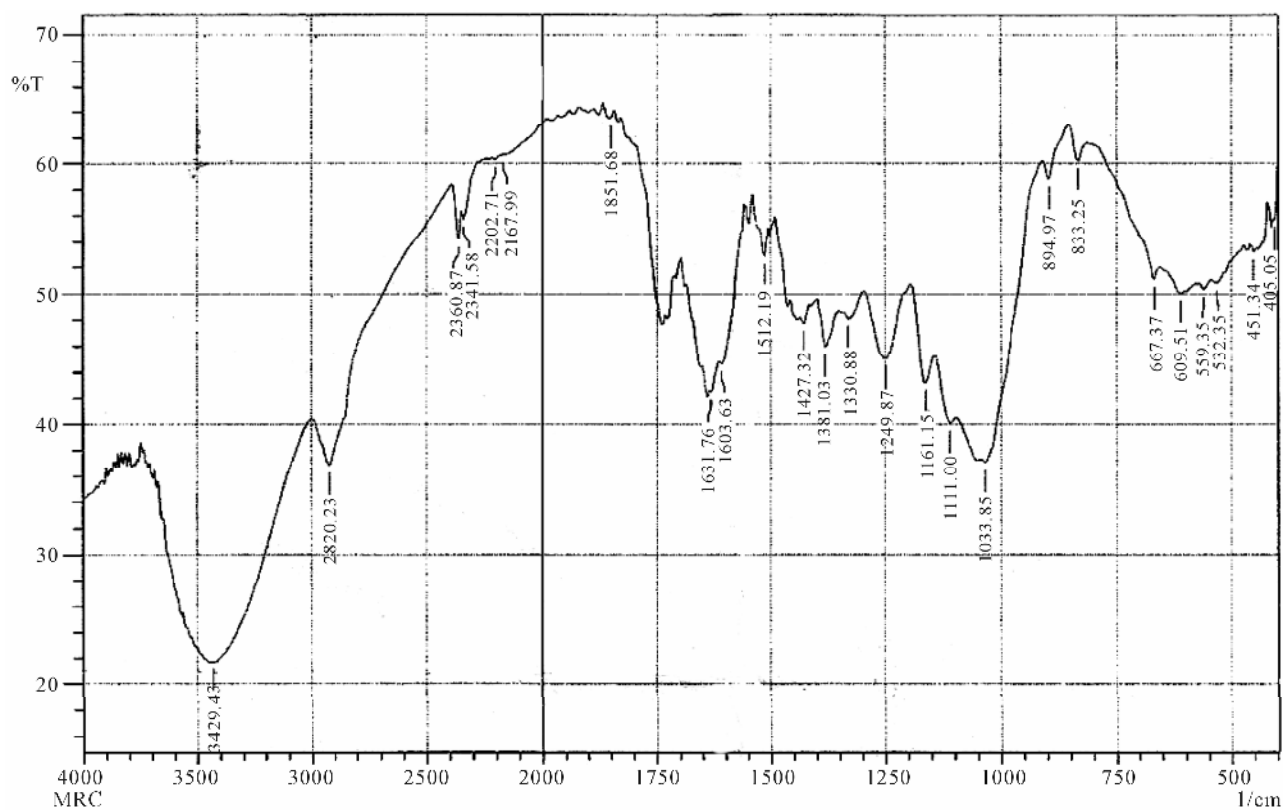
Scanning electron microscopy was used to study the surface morphology and the pore size of the samples. Samples of MRC and ZRC were subjected to SEM studies and SEM micrograph (**Figures 5(a)** and **(b)**) shows many orderly and developed pores.

It can be seen from the micrographs that the external surface of ZRC is full of cavities compared with MRC, and quite irregular as a result of activation and the pores were different sizes and different shapes. According to the micrograph, it seems that the cavities resulted from the evaporation of $ZnCl_2$ during carbonization, leaving the space previously occupied by the $ZnCl_2$. It is clear that the adsorbent has considerable number of heterogeneous pores where there is a good possibility for dye to be trapped and adsorbed [27].

Based on the EDAX results, the elementary analysis of



(a)



(b)

Figure 4. FTIR spectra of (a) MRC and (b) ZRC.

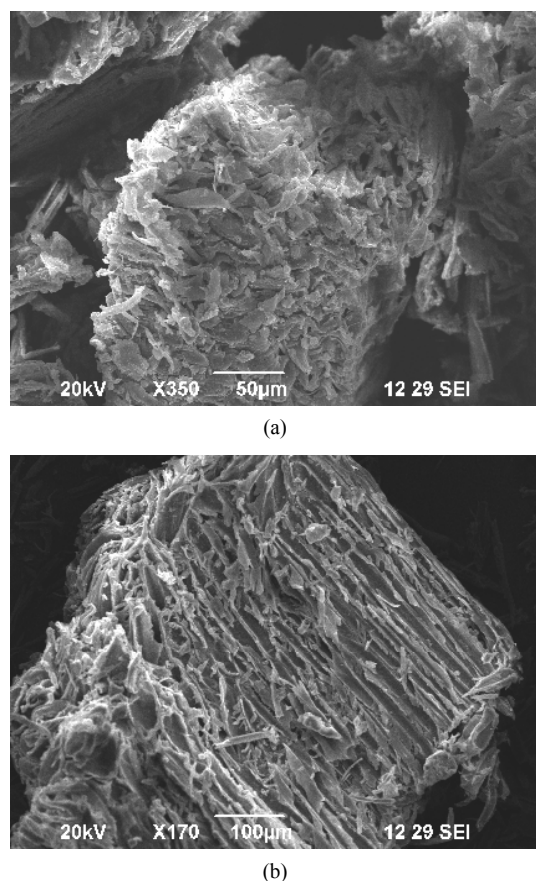


Figure 5. SEM images of (a) MRC and (b) ZRC.

the MRC and ZRC are presented in the **Figures 6(a)** and **(b)**. The elements, percentage mass of elements presented in MRC and ZRC are summarized in **Tables 3** and **4**.

3.5. Effect of Solution pH on MG Dye Adsorption

The effect of solution pH is very important when the adsorbing molecules are capable of ionizing in response to the current pH [24]. The uptake of MG from aqueous solution was greatly affected by the variation of pH value, as shown in **Figure 7**. When the pH was lower than 3, the uptake went up sharply with the increase of pH. The maximum MG uptake was obtained at pH = 5. At the initial dye concentration of 100 mg/L, removal efficiency was 19.43%, 36.10% at a solution pH of 2.0 for MRC and ZRC, respectively, but it increased when solution pH increases from 2 to 5. At pH 5, the removal efficiency was 48.58%, 63.56% for MRC and ZRC, respectively.

The optimum pH value for the adsorption of MG onto MRC and ZRC (pH = 5) was observed. That may be attributed to the hydrophobic nature of the developed carbon which led to absorb hydrogen ions (H^+) onto the surface of the carbon when immersed in water and make

Table 3. Data for the elements presented in MRC.

Element	(keV)	Mass %	Atom %	K
C K	0.277	81.56	87.06	1
O K	0.525	14.55	11.66	0.3805
K K	3.312	3.89	1.28	0.4333
Total		100	100	

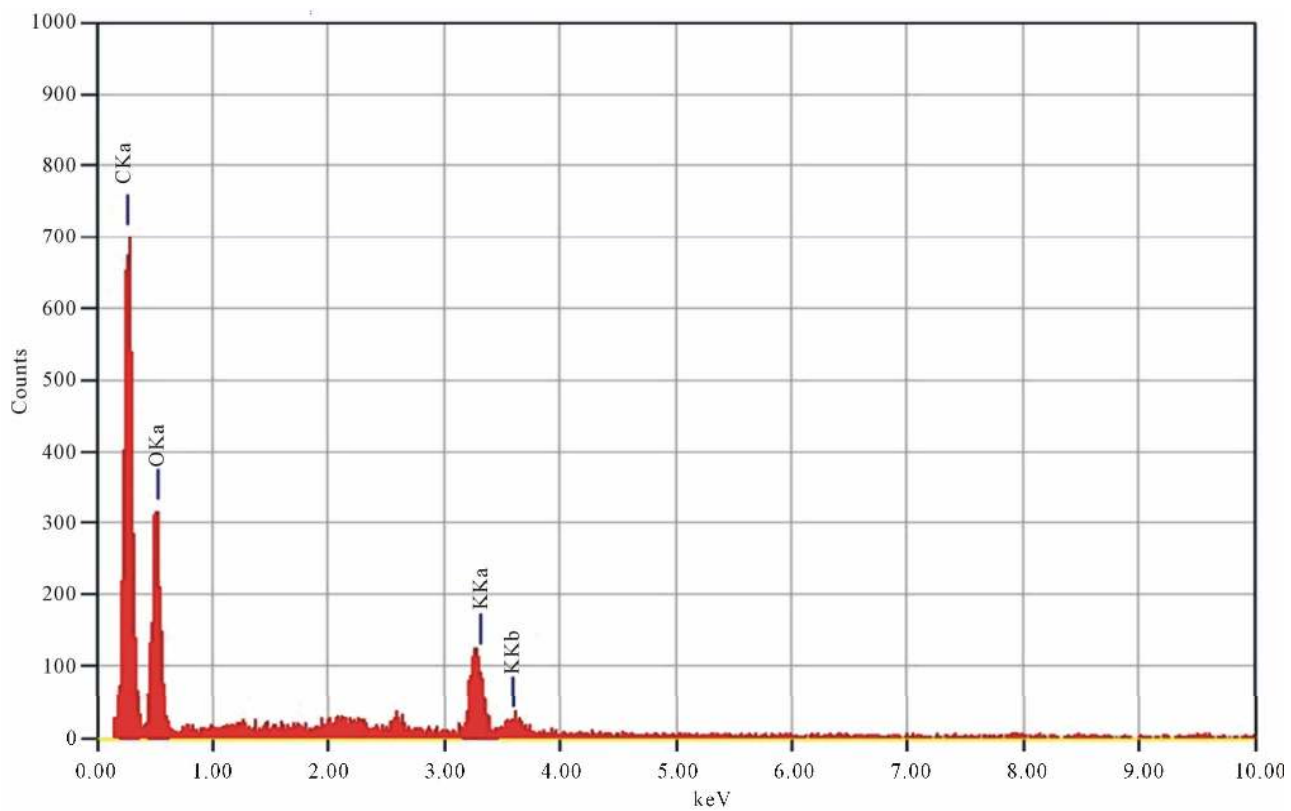
Table 4. Data for the elements presented in ZRC.

Element	(keV)	Mass %	Atom %	K
C K	0.277	76.02	84.53	1
O K	0.525	16.76	14	0.3805
Zn L	1.012	7.22	1.47	1.2304
Total		100	100	

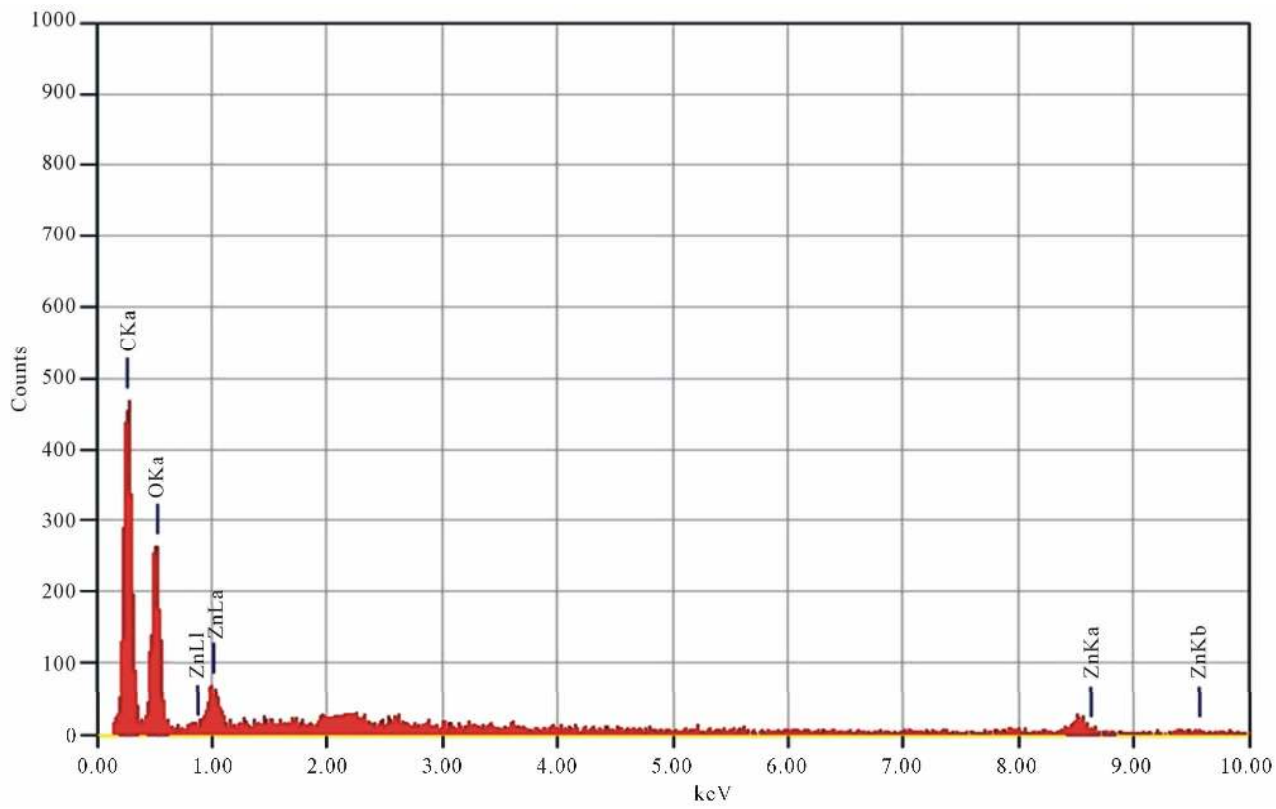
it positively charged. Low pH value (1.0 to 4.0) leads to an increase in H^+ ion concentration in the system and the surface of the activated carbon acquires positive charge by absorbing H^+ ions. On the other hand, increase of the pH value led to increase of the number of negatively charged sites. As the adsorbent surface is negatively charged at high pH, a significantly strong electrostatic attraction appears between the negatively charged carbon surface and cationic dye molecule leading to maximum adsorption of MG from waste water [28]. The lowest adsorption occurred at pH 2.0 and the greatest adsorption occurred at pH ~ 5.0. Adsorbents surface would be positively charged up to pH < 4, and heterogeneous in the pH range 4 - 5, thereafter it should be negatively charged. Moreover, the increasing in the adsorption of dye with increasing of pH value is also due to the attraction between cationic dye and excess OH^- ions in the solution [29]. When solution pH increases, high OH^- ions accumulate on the adsorbent surface [30]. Therefore, electrostatic interaction between negatively charged adsorbent surface and cationic dye molecule caused the increase in adsorption. Furthermore, the solution pH is above the zero point of charge (pH_{zpc} , 3.14 for MRC and pH_{zpc} , 4.0 for ZRC) and hence the negative charge density of the surface of the adsorbents were increased which favors the adsorption of cationic dye [22].

3.6. Effect of Adsorbent Dose on MG Adsorption

The adsorbent dose is an important parameter in adsorption studies because it determines the capacity of adsorbent for a given initial dye concentration of dye solution. The effect of adsorbent dose on MG dye removal percentage is shown in **Figure 8**. The effect of adsorbent dose was observed by keeping the optimum pH at equi-



(a)



(b)

Figure 6. EDAX spectra of (a) MRC and (b) ZRC.

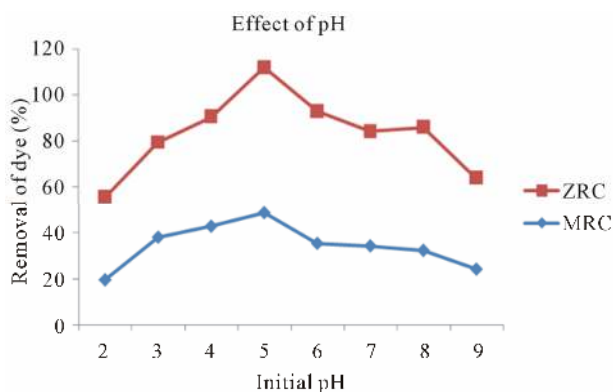


Figure 7. Effect of pH on the adsorption of MG onto MRC and ZRC.

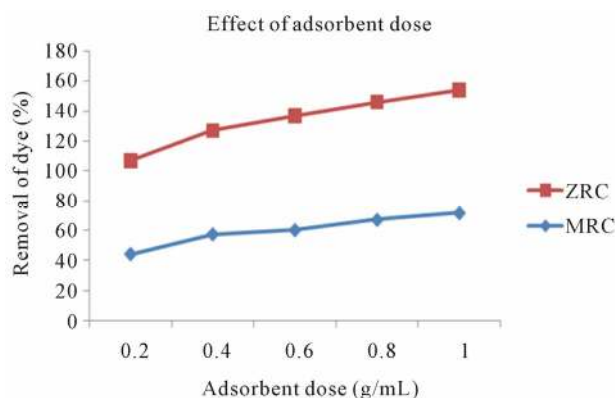


Figure 8. Effect of adsorbent dose on the removal of MG onto MRC and ZRC (MG concentration 100 mg/L, contact time 2 h, solution pH 5).

librium times for each adsorption process. It was observed that the percentage of adsorption increases with increase in adsorbent dose from 0.2 g to 1 g in MG with the concentration of dye solution of 100 mg/L. The increase in % dye removal was due to the increase of the available sorption surface and availability of adsorption sites [31]. A similar observation was previously reported for the removal of malachite green dye from aqueous solution by bagasse fly ash and activated carbon [32]. Therefore, 0.2 g/mL of adsorbent was chosen for later studies on MG adsorption.

3.7. Effect of Initial MG Dye Concentration

The data for the uptake of MG onto MRC and ZRC as a function of initial dye concentration is presented in **Figure 9**. It can be seen (**Figure 9**) that the amount of MG adsorbed per unit mass of adsorbent increased with the increase in initial concentration and attained saturation after equilibrium time, although percentage removal decreased with the increase in initial concentration. The percentage removal shows that, with an increase in the initial concentration of dyes, the percent removal was

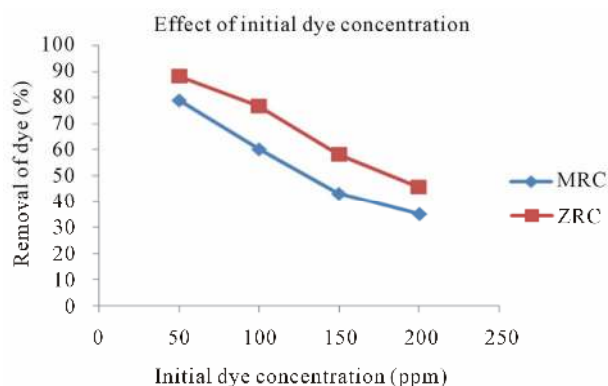


Figure 9. Effect of Initial dye concentration on the removal of MG onto MRC and ZRC (adsorbent dose 0.2 g/L, contact time 2 h, solution pH 5).

decreased from 79.10% to 35.04% (MG onto MRC), 88.24% to 55.60% (MG onto ZRC) for the dye concentration of 50 to 200 mg/L.

This may be attributed to an increase in the driving force of the concentration gradient with increase in the initial dye concentration [33,34].

3.8. Adsorption Isotherm Studies for MG in Single System

The Langmuir, Freundlich, Temkin and Dubinin-Radushkevich isotherm models were used to describe the relationship between the amount of MRC, ZRC adsorbed and its equilibrium concentration in solutions.

Langmuir [35] proposed a theory to describe the adsorption of gas molecules onto metal surfaces. The Langmuir adsorption isotherm has been successfully applied to many real sorption processes. Langmuir isotherm model assumes uniform energies of adsorption onto the surface without transmigration of adsorbate in the plane of the surface [36]. Therefore, the Langmuir isotherm model was chosen for the estimation of maximum adsorption capacity corresponding to complete monolayer coverage on the adsorbent surface. The Langmuir nonlinear equation is commonly expressed as:

$$q_e = \frac{Q_m K_L C_e}{1 + K_L C_e} \quad (3)$$

In Equation (3), C_e and q_e are defined as before in Equation (2), Q_m is a constant and reflect a complete monolayer coverage (mg/g), K_L is adsorption equilibrium constant (L/mg) that is related to the apparent energy of sorption. Langmuir isotherm [37] assumes monolayer adsorption onto a surface containing a finite number of adsorption sites. The Langmuir isotherm Equation (3) can be linearized into the following form [38,39]:

$$\frac{C_e}{q_e} = \frac{1}{K_L Q_m} + \frac{1}{Q_m} \times C_e \quad (4)$$

A plot of C_e/q_e versus C_e should indicate a straight line slope of $1/Q_m$ and an intercept of $1/K_L Q_m$. **Table 5** shows the values of the correlation coefficient (R^2), sorption capacity (Q_m), and sorption energy (n) calculated from the plot indicated in **Figure 10**. The correlation coefficient (R^2) for the adsorption of MG onto MRC (S) and ZRC (S) is equal to 0.990 and 0.9960, showing a favorable adsorption of MG onto MRC and ZRC in single system (S).

The value of Q_m obtained was equal to 12.65 mg/g and 24.39 mg/g for MRC (S) and ZRC (S), indicating a very strong monolayer adsorption of the adsorbate on the surface.

The Freundlich isotherm is an empirical equation assuming that the adsorption process takes place on a heterogeneous surface through a multilayer adsorption mechanism and adsorption capacity is related to the concentration of dye at equilibrium [40]. The Freundlich equation is given as:

$$q_e = K_f C_e^{1/n} \quad (5)$$

where q_e is the amount of adsorbate at equilibrium (mg/g), C_e is the equilibrium concentration of the adsorbate (mg/L), K_f is the Freundlich adsorption constant

Table 5. Adsorption isotherm parameters of MG in single and binary system.

Isotherm model	MRC (S)	MRC (B)	ZRC (S)	ZRC (B)
Langmuir				
Q_m (mg·g ⁻¹)	12.6500	11.7647	24.3900	20.4081
b (L·mg ⁻¹)	0.2041	0.0850	0.0073	0.0491
R^2	0.9900	0.9800	0.9960	0.9790
Freundlich				
$1/n$	0.0590	0.3570	0.2820	0.3740
K_f (mg·g ⁻¹)	8.9000	3.7325	5.9000	2.2542
R^2	0.8860	0.9140	0.9780	0.9690
Dubinin-Radushkevich				
Q_m (mg·g ⁻¹)	11.7230	10.6400	19.8000	18.177
K ($\times 10^{-5}$ mol ² ·kJ ⁻²)	1.0000	2.0000	1.0000	1.0000
E (kJ·mol ⁻¹)	0.0709	0.1581	0.0707	1.0000
R^2	0.6390	0.9370	0.8350	0.9600
Temkin				
α (L·g ⁻¹)	3.2060	0.1191	2.6050	0.3112
β (mg·L ⁻¹)	0.6660	4.7280	4.3420	0.7370
b	349.53	52.7530	53.614	235.58
R^2	0.8690	0.9400	0.9890	0.9590

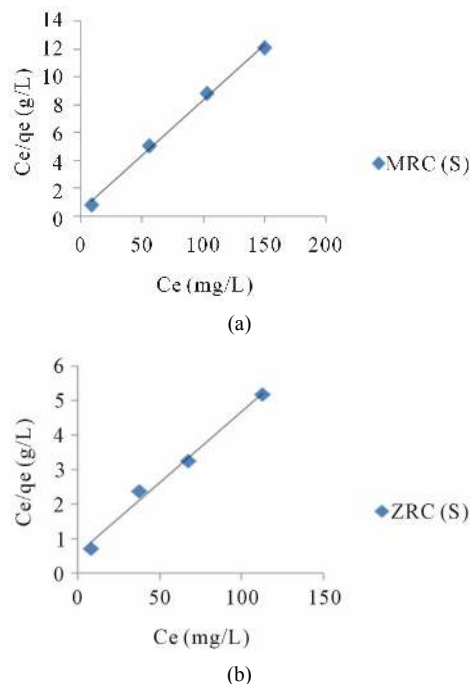


Figure 10. Langmuir adsorption isotherm for MG onto (a) S-MRC and (b) S-ZRC.

related to adsorption capacity of the adsorbent and $1/n$ is the adsorption intensity. A linear form of the Freundlich equation is generally expressed as follows:

$$\ln q_e = \ln K_f + \frac{1}{n} \ln C_e \quad (6)$$

The values of K_f and $1/n$ were calculated from the intercept and slope of the plot of $\ln q_e$ versus $\ln C_e$. **Table 5** shows the calculated Freundlich parameters. The coefficient K_f , correlation coefficient (R^2) was slightly less than that of Langmuir isotherm and, consequently, was a less favorable adsorption.

The *Dubinin-Radushkevich* equation can be expressed [41] as:

$$q_e = q_m e^{-K'\varepsilon^2} \quad (7)$$

where ε (Polanyi potential) is equal to $RT \ln(1 + 1/C_e)$, q_e is the amount of the dye adsorbed per unit activated carbon (mol/g), q_m the theoretical monolayer saturation capacity (mol/g), C_e the equilibrium concentration of the dye solution (mol/L), K' is the constant of the adsorption energy (mol²/kJ²), R is the gas constant (8.314 KJ/mol K), and T is the temperature (K). The linear form of the D-R isotherm is:

$$\ln q_e = \ln q_m - k'\varepsilon^2 \quad (8)$$

K' is related to mean adsorption energy E (kJ/mol) as [42]:

$$E = \frac{1}{\sqrt{2K^{-1}}} \quad (9)$$

The calculated D-R adsorption isotherm parameters should be summarized in **Table 5**.

Temkin and Pyzhev considered the effects of some indirect sorbate/adsorbate interactions on adsorption isotherms, and suggest that the heat of adsorption of all the molecules in the layer would decrease linearly with coverage due to these interactions [43]. The Temkin isotherm has been used in the following form:

$$q_e = \frac{RT}{b} \ln(K_T C_e) \quad (10)$$

where K_T is the equilibrium binding constant (L/g), b is related to heat of adsorption (J/mol), R is the universal gas constant (8.314 J/mol K) and T is the absolute temperature (K). Equation (10) can be written as the following form:

$$q_e = B_1 \ln(K_T C_e) \quad (11)$$

The Temkin adsorption isotherm parameters are calculated and the values are summarized in **Table 5**.

Adsorption isotherms describe the interaction of adsorbates with the adsorbent materials, and thus are critical for optimization of the adsorption mechanism pathways [44]. Therefore, the correlation of equilibrium data by the empirical equations is essential to the practical design and operation of adsorption systems [45]. The experimental data of MG dye were modeled using Langmuir, Freundlich, Temkin and Dubinin-Radushkevich isotherm models. Isotherm parameters for the adsorption of MG onto MRC and ZRC in single (S) and binary system (B) were summarized in **Table 5**. The applicability of Langmuir isotherm model suggests that the adsorption takes place on homogeneous sites within the adsorption site (the adsorbed layer is one molecule in thickness), with each molecule possess constant enthalpies and sorption activation energy. The results also demonstrate there is no interaction and transmigration of dyes in the plane of the neighboring surface.

3.9. Adsorption Kinetics

The kinetics describes the rate of adsorbate uptake on activated carbon. In order to identify the potential rate controlling steps involved in the process of adsorption, four kinetic models were studied and used to fit the experimental data from the adsorption of MG dye onto MRC and ZRC. These models are the pseudo-first-order, pseudo-second-order, Elovich and intra-particle kinetic models.

3.9.1. Pseudo-First-Order Kinetic Model

The pseudo first-order equation of Lagergren is generally expressed as follows [46,47]:

$$\frac{dq_t}{dt} = K_1 (q_e - q_t) \quad (12)$$

After integration and applying boundary conditions, $t = 0$ to $t = t$ and $q_t = 0$ to $q_t = qt$; the integrated form of the above equation becomes:

$$q_t = q_e (1 - e^{-K_1 t}) \quad (13)$$

However, Equation (13) is transformed into its linear form for use in the kinetic analyses of data can be expressed as:

$$\ln(q_e - q_t) = \ln q_e - K_1 t \quad (14)$$

where q_e (mg/g) and q_t (mg/g) are the amount of adsorbed adsorbate at equilibrium and at time t , respectively, and k_1 (1/min) is the rate constant of pseudo first-order adsorption. The straight line plots of $\log(q_e - q_t)$ against t of Equation (14) were made.

The data for the pseudo-first-order kinetic model of MG onto MRC (S) and ZRC (S) are summarized in **Table 6**. In order to obtain the rate constants, the values of $\log(q_e - q_t)$ were linearly correlated with time. The plot of $\log(q_e - q_t)$ versus time gives a linear relationship from which k_1 and predicted q_e can be determined from the slope and intercept of the plot. The K_1 values, correlation coefficient values and q_e values (experimental and calculated) are summarized in **Table 6**. The correlation coefficient R^2 is relatively low for the adsorption data. Besides, the experimental q_e values, did not agree with the calculated values obtained from the linear plots. It suggests that the kinetics of MG onto MRC and ZRC did not follow the pseudo-first-order kinetic model.

3.9.2. Pseudo-Second-Order Kinetic Model

The rate of sorption is a second-order mechanism, the pseudo-second-order chemisorptions kinetic rate equation is expressed as:

$$\frac{t}{q_t} = \frac{1}{K q_e^2} + \frac{1}{q_e} t \quad (15)$$

where q_e and q_t are the sorption capacities at equilibrium and at time t , respectively (mg/g) and k is the rate constant of pseudo-second-order sorption (g/mg/min). Where h can be regarded as the initial sorption rate as q_t/t tends to zero, hence:

$$h = k q_e^2 \quad (16)$$

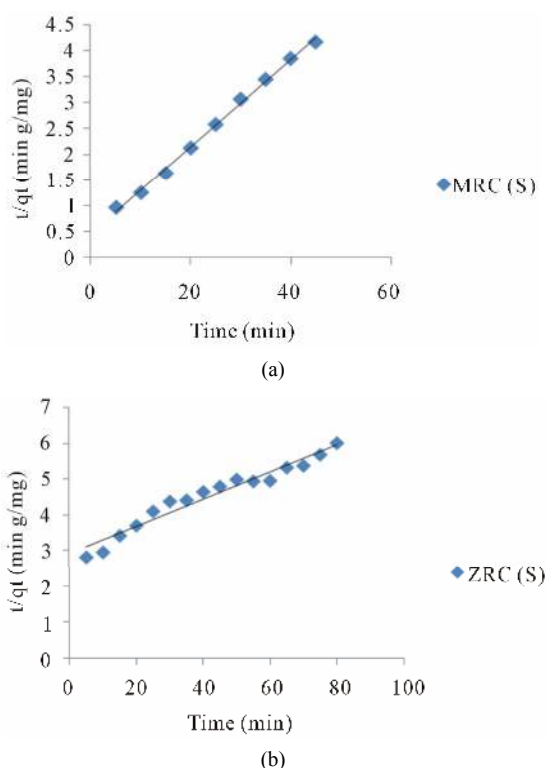
Equation (16) can be written as:

$$\frac{t}{q_t} = \frac{1}{h} + \frac{1}{q_e} \times t \quad (17)$$

Equation (16) does not have the disadvantage of the problem with assigning an effective q_e . If Pseudo-second-order kinetics are applicable, the plot of t/q_t against t of Equation (17) should give a linear relationship, from which q_e , k and h can be determined from the slope and intercept of the plot (**Figure 11**) and there is no need to

Table 6. Comparison of the correlation coefficients of kinetic parameters for MG adsorption onto MRC and ZRC in single and binary system.

Models	Parameters	MRC (S)	ZRC (S)	MRC (B)	ZRC (B)
Pseudo first-order model	k_1 (min^{-1})	0.0492	0.0382	0.0391	0.0420
	q_e (mg/g)	14.4565	28.913	4.6558	5.6720
	R^2	0.7700	0.8713	0.9350	0.9180
Pseudo second-order model	k_2 (g/mg/min)	0.0671	0.0593	0.0085	7.9103
	q_e (mg/g)	11.9047	23.8095	9.9047	11.3457
	h	2.1400	0.9963	13.6979	4.4840
Intra particle diffusion model	R^2	0.9900	0.9967	0.9620	0.9870
	K_{dif} (mg/(g·min ^{1/2}))	1.0354	2.5882	0.0650	0.5750
	C	4.2120	8.1679	0.1500	15.6400
Elovich model	R^2	0.8389	0.9862	0.9830	0.9260
	A_E (mg(g/min))	0.4310	0.1660	5.4645	1.7636
	b (g/mg)	0.2004	0.1979	2.5616	7.5863
	R^2	0.9380	0.8154	0.6410	0.5640

**Figure 11. Pseudo-second-order kinetics for the adsorption of MG onto (a) S-MRC and (b) S-ZRC.**

know any parameter. The q_e and k_2 values were estimated from the slope ($1/q_e$) and intercept ($1/k_2 q_e^2$) of linear plot of t/q_t versus t .

The data for the pseudo-second-order kinetic model of

MG onto MRC (S) and ZRC (S) are summarized in **Table 6**. The corresponding correlation coefficient (R^2) values for the pseudo-second-order kinetic model were 0.9900 for MRC (S) and 0.9967 for ZRC (S), respectively, indicates the applicability of the pseudo-second-order kinetic model to describe the adsorption process of MG onto MRC and ZRC. This led to believe that the pseudo-second-order kinetic model provided good correlation for the adsorption. The higher R^2 values confirm that the sorption process of dyes onto MRC and ZRC follow a pseudo-second-order kinetic model. Similar trends were observed for dye adsorption onto *Zea mays* (maize) cob [48], for adsorption onto ginger waste [30]. It suggested that the adsorption process was controlled by chemisorption process [31].

3.9.3. Intra Particle Diffusion Model

The adsorption of MG dye onto MRC (S) and ZRC (S) may be controlled by via external film diffusion at earlier stages and later by the particle diffusion. The possibility of intra particle diffusion resistance was identified by using the following intra particle diffusion model as [49]:

$$q_t = K_{\text{dif}} t^{1/2} + C \quad (18)$$

where K_{dif} is the intra-particle diffusion rate constant ($\text{mg}/(\text{g}\cdot\text{min}^{1/2})$), C is the intercept. The values of q_t correlated linearly with the values of $t^{1/2}$ and the rate constant K_{dif} directly evaluated from the slope of regression line. The data for the intra-particle kinetic model of MG onto MRC (S) and ZRC (S) are summarized in **Table 6**.

The linearity of the plots demonstrated that intra-par-

tion diffusion played a significant role in the uptake of the MG onto MRC and ZRC. However, as still there is no sufficient indication about it, Ho [50] has shown that if the intra-particle diffusion is the sole rate-limiting step, it is essential for the q_t versus $t^{1/2}$ plots to pass through the origin, which is not the case, it may be concluded that surface adsorption and intra-particle diffusion were concurrently operating during the MRC and ZRC interactions. Hence intra-particle diffusion is not a fully operative mechanism in the sorption of MG onto MRC and ZRC.

3.9.4. Elovich Kinetics

The Elovich kinetic is another rate equation based on the adsorption capacity generally expressed as follows:

$$\frac{dq_t}{dt} = B_E e^{-(A_E q_t)} \quad (19)$$

where B_E is the initial adsorption rate constant (mg (g/min) and A_E is the desorption constant (g/mg) during any experiment.

It is simplified by assuming $A_E B_E t \gg t$ and by applying the boundary conditions $q_t = 0$ at $t = 0$ and $q_t = t$ at $t = t$ above Equation (19) becomes:

$$q_t = \frac{1}{A_E} (B_E A_E) + \frac{1}{A_E} \ln t \quad (20)$$

If MG adsorption by MRC and ZRC fits the Elovich model, a plot of q_t versus $\ln(t)$ should yield a linear relationship with a slope of $(1/A_E)$ and an intercept of $(1/A_E) \ln(A_E B_E)$. Thus the constants can be obtained from the slope and the intercept of the straight line.

Thus, the constants can be obtained from the slope and the intercept are shown in **Table 6**. The parameter $1/A_E$ is related to the number of sites available for adsorption while $(1/A_E) \ln(A_E B_E)$ is the adsorption quantity when $\ln t$ is equal to zero; ie, the adsorption quantity when t is 1 min. This value is helpful in understanding the adsorption behavior of the first step [51]. In the case of using the Elovich equation, the correlation coefficients are lower than those of pseudo-second-order equation. The Elovich equation does not predict any definite mechanism, but it is useful in describing adsorption on highly heterogeneous adsorbents.

The correlation coefficients obtained for the pseudo-second-order kinetic model are greater than 0.93 for MRC (S) and ZRC (S). The theoretical q_t values of the pseudo-second-order kinetic model for MRC (S) and ZRC (S) are close to the experimental values than those of the other models. The pseudo-second-order kinetic model fits the experimental data better than the other kinetic models in this study.

The Langmuir isotherm and pseudo-second-order kinetic model provide best correlation with the experimen-

tal data for the adsorption of MG onto MRC and ZRC for different initial dye concentrations over the whole range studied. Both Langmuir isotherm and pseudo-second-order kinetic model assumes that the MRC and ZRC surface is homogenous and the operating adsorption mechanism is chemisorptions process.

3.10. The Competitive Adsorption of MG in Binary System

Effects of the presence of MRC and ZRC on the adsorption of MG were investigated in terms of equilibrium isotherm and adsorption kinetics. A comparison of the adsorbed quantity of MG onto MRC and ZRC in single system at equilibrium between the solutions with MG present in the binary system (B) was given in **Figure 12**. As shown in **Figure 12**, the results indicated that the equilibrium uptake of MG onto MRC and ZRC in single and binary systems.

All the correlation coefficient, R^2 values and the constants obtained from the four isotherm models and four kinetic models are summarized in **Tables 5** and **6**. The Langmuir isotherm model gave the highest R^2 values. Among the four kinetic models pseudo-second-order model fits well for MG adsorption onto MRC and ZRC in single and binary system. In the single dye solution, the maximum uptake obtained at initial concentrations of MG 100 mg/L, pH 5 was found to be 12.65 mg/g for MRC (S) and 24.39 mg/g for ZRC (S), while the uptake obtained in the binary solutions at the same initial dye concentration of MG and adsorption conditions, was found to be 11.764 mg/g for MRC (B) and 20.4081 mg/g for ZRC (B), respectively.

A fixed quantity of MG onto MRC (S) and ZRC (S) could only offer a finite number of surface binding sites, some of which would be expected to be saturated by the competing dye solutions. The decrease in sorption capacity of same activated carbon in target dye solution than that of single (S) dye may be ascribed to the less availability of binding sites. In case of binary dye (B) solution,

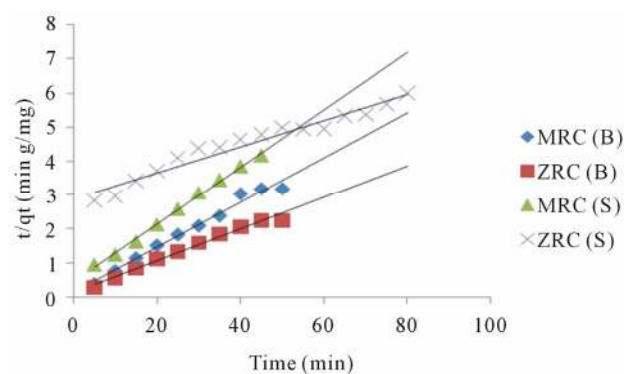


Figure 12. Comparison of pseudo-second-order kinetics of MG in single and binary solutions onto MRC and ZRC.

the binding site is competitively divided among the various dye solutions.

Among MRC and ZRC, ZRC shows most adsorption ability than MRC in single system only onto MG adsorption from waste water using epicarp of *Ricinus communis*.

4. Conclusion

It had indicated that $ZnCl_2$ was a suitable activating agent for the preparation of activated carbon from epicarp of *Ricinus communis* by microwave radiation. The effects of the impregnation ratio of $ZnCl_2$, microwave radiation power and microwave radiation time and impregnation time on the yield and iodine number of ZRC were investigated systematically. The optimum conditions were microwave power of 100 W, microwave radiation time of 4 min, concentration of zinc chloride of 30% by volume and impregnation time of 16 h. SEM micrographs showed that the external surface of the chemically activated carbon was full of cavities compared with untreated *Ricinus communis*. The activated carbon prepared could effectively used as adsorbent for the removal of basic dye from aqueous solutions. Adsorption was found to be maximum in the pH of 5. Langmuir isotherm models given were fitting better than Freundlich, Temkin and Dubinin-Radushkevich isotherms interpreting the adsorption phenomenon of MG. MG adsorption system follows pseudo-second-order kinetic model, based on the assumption that the rate-limiting step may be chemisorptions process. MG adsorption rate onto MRC and ZRC was greater in single system (S) than in binary system (B) due to the competitive adsorption of dye onto the active site of the activated carbon. Among MRC and ZRC, ZRC shows most adsorption ability than MRC in single and binary system.

REFERENCES

- [1] S. M. A. G. U. de Souza, L. C. Peruzzo and A. A. U. de Souza, "Numerical Study of the Adsorption of Dyes from Effluents," *Applied Mathematical Modelling*, Vol. 32, No. 9, 2008, pp. 1711-1718. doi:10.1016/j.apm.2007.06.007
- [2] K. V. Kumar, S. Sivanesan and V. Ramamurthi, "Adsorption of Malachite Green onto *Pithopora* sp., a Fresh Water Algal: Equilibrium and Kinetic Modeling," *Process Biochemistry*, Vol. 40, No. 48, 2005, pp. 2865-2872. doi:10.1016/j.procbio.2005.01.007
- [3] V. K. Gupta, A. Mittal, L. Krishnan and V. Gajbe, "Adsorption Kinetics and Column Operations for the Removal and Recovery of Malachite Green from Wastewater Using Bottom Ash," *Separation and Purification Technology*, Vol. 40, No. 1, 2004, pp. 87-96. doi:10.1016/j.seppur.2004.01.008
- [4] M.-S. Chiou and H.-Y. Li, "Equilibrium and Kinetic Modeling of Adsorption of Reactive Dyes on Cross-Linked chitosan Beads," *Journal of Hazardous Materials*, Vol. 93, No. 2, 2002, pp. 233-248. doi:10.1016/S0304-3894(02)00030-4
- [5] O. S. Bello, M. A. Ahmad and T. S. Tan, "Utilization of Cocopod Husk for the Removal of Remazol Black B Reactive Dye from Aqueous Solutions: Kinetic, Equilibrium and Thermodynamic Studies," *Trends in Applied Sciences Research*, Vol. 6, No. 8, 2011, pp. 794-812. doi:10.3923/tasr.2011.794.812
- [6] B. H. Hameed, A. L. Ahmad and K. N. A. Latiff, "Adsorption of Basic Dye (Methylene Blue) onto Activated Carbon Prepared from Rattan Sawdust," *Dyes and Pigments*, Vol. 75, No. 1, 2007, pp. 143-149. doi:10.1016/j.dyepig.2006.05.039
- [7] U. Kumar and M. Bandyopadhyay, "Sorption of Cadmium from Aqueous Solution Using Pretreated Rice Husk," *Bioresource Technology*, Vol. 97, No. 1, 2006, pp. 104-109. doi:10.1016/j.biortech.2005.02.027
- [8] K. V. Kumar, "Optimum Sorption Isotherm by Linear and Nonlinear Methods for Malachite onto Lemon Peel," *Dyes and Pigments*, Vol. 74, No. 3, 2007, pp. 595-597. doi:10.1016/j.dyepig.2006.03.026
- [9] R. M. Gong, X. P. Zhang, H. J. Liu, Y. Z. Sun and B. R. Liu, "Uptake of Cationic Dyes from Aqueous Solution by Biosorption onto Granular Kohlrabi Peel," *Bioresource Technology*, Vol. 98, No. 6, 2007, pp. 1319-1323. doi:10.1016/j.biortech.2006.04.034
- [10] S. Senthilkumar, P. R. Varadarajan, K. Porkodi and C. V. Subhuraam, "Adsorption of Methylene Blue onto Jute Fibre Carbon; Kinetics and Equilibrium Studies," *Journal of Colloid and Interface Science*, Vol. 284, No. 1, 2005, pp. 78-82. doi:10.1016/j.jcis.2004.09.027
- [11] I. A. W. Tan, L. Ahmad and B. H. Hameed, "Optimization of Preparation Conditions for Activated Carbons from Coconut Husk Using Response Surface Methodology," *Journal of Chemical Engineering*, Vol. 137, No. 3, 2008, pp. 462-470. doi:10.1016/j.ccej.2007.04.031
- [12] J. Hayashi, A. Kazehaya, K. Muroyama and A. P. Watkinson, "Preparation of Activated Carbon from Lignin by Chemical Activation," *Carbon*, Vol. 38, No. 13, 2008, pp. 1873-1878. doi:10.1016/S0008-6223(00)00027-0
- [13] M. M. Karim, A. K. Das and S. H. Lee, "Treatment of Colored Effluent of the Textile Industry in Bangladesh Using Zinc Chloride Treated Indigenous Activated Carbons," *Journal of Analytical Chemistry*, Vol. 576, No. 1, 2006, pp. 37-42. doi:10.1016/j.aca.2006.01.079
- [14] C. Almansa, M. Molina-Sabio and F. Rodriguez-Reinso, "Adsorption of Methane into $ZnCl_2$ -Activated Carbon Derived Discs," *Journal of Microporous and Mesoporous Materials*, Vol. 76, No. 1-3, 2004, pp. 185-191. doi:10.1016/j.micromeso.2004.08.010
- [15] W. Li, L.-B. Zhang, J.-H. Peng, N. Li and X.-Y. Zhang, "Preparation of High Surface Area Activated Carbons from Tobacco Stems with K_2CO_3 Activation Using Microwave Radiation," *Journal of Industrial Crops and Products*, Vol. 27, No. 3, 2008, pp. 341-347. doi:10.1016/j.indcrop.2007.11.011
- [16] C. O. Ania, J. B. Parra, J. A. Menendez and J. J. Pis, "Ef-

- fect of Microwave and Conventional Regeneration on the Microporous and Mesoporous Network on the Adsorptive Capacity of Activated Carbons,” *Journal of Microporous and Mesoporous Materials*, Vol. 63, No. 1-2, 2005, pp. 7-15. [doi:10.1016/j.micromeso.2005.06.013](https://doi.org/10.1016/j.micromeso.2005.06.013)
- [17] J. M. V. Nabais, P. J. M. Carrot, M. M. L. R. Carrott and J. A. Menendez, “Preparation and Modification of Activated Carbon Fibres by Microwave Heating,” *Carbon*, Vol. 42, No. 7, 2004, pp. 1315-1320. [doi:10.1016/j.carbon.2004.01.033](https://doi.org/10.1016/j.carbon.2004.01.033)
- [18] D. A. Jones, T. P. Leyveld, S. D. Mavrofidis, S. W. Kingman and N. J. Miles, “Microwave Heating Applications in Environmental Engineering: A Review,” *Resources, Conservation and Recycling*, Vol. 34, No. 2, 2002, pp. 75-90. [doi:10.1016/S0921-3449\(01\)00088-X](https://doi.org/10.1016/S0921-3449(01)00088-X)
- [19] T. Santhi, S. Manonmani and T. Smitha, “The Removal of Malachite Green from Aqueous Solution by Activated Carbon Prepared from the Epicarp of Ricinus Communis by Adsorption,” *Journal of Hazardous Materials*, Vol. 179, No. 1-3, 2010, pp. 178-186. [doi:10.1016/j.jhazmat.2010.02.076](https://doi.org/10.1016/j.jhazmat.2010.02.076)
- [20] A. Kumar, B. Prasad and I. M. Mishra, “Adsorptive Removal of Acrylonitrile by Commercial Grade Activated Carbon: Kinetics, Equilibrium and Thermodynamics,” *Journal of Hazardous Materials*, Vol. 152, No. 2, 2008, pp. 589-600. [doi:10.1016/j.jhazmat.2007.07.048](https://doi.org/10.1016/j.jhazmat.2007.07.048)
- [21] H. P. Boehm, “Surface Oxides on Carbon and Their Analysis: A Critical Assessment,” *Carbon*, Vol. 40, No. 2, 2002, pp. 145-149. [doi:10.1016/S0008-6223\(01\)00165-8](https://doi.org/10.1016/S0008-6223(01)00165-8)
- [22] P. Janos, H. Buchtova and M. Ryznarova, “Sorption of Dye from Aqueous Solution onto Fly Ash,” *Water Research*, Vol. 37, No. 20, 2003, pp. 4938-4944. [doi:10.1016/j.watres.2003.08.011](https://doi.org/10.1016/j.watres.2003.08.011)
- [23] S. D. Khattri and M.K. Singh, “Removal of Malachite Green from Dye Wastewater Using Neem Sawdust by Adsorption,” *Journal of Hazardous Materials*, Vol. 167, No. 1-3, 2009, pp. 1089-1094. [doi:10.1016/j.jhazmat.2009.01.101](https://doi.org/10.1016/j.jhazmat.2009.01.101)
- [24] B. K. Hamad, A. M. Noor, A. R. Afida and M. N. M. Asri, “High Removal of 4-Chloroguaiacol by High Surface Area of Oil Palm Shell-Activated Carbon Activated with NaOH from Aqueous Solution,” *Desalination*, Vol. 257, No. 1-3, 2010, pp. 1-7. [doi:10.1016/j.desal.2010.03.007](https://doi.org/10.1016/j.desal.2010.03.007)
- [25] A. Reffas, V. Bernardet, B. David, L. Reinerts, M. B. Lehocine, M. D. Batisse and L. Duciaux, “Carbon Prepared from Coffee Grounds by H₃PO₄ Activation: Characterization and Adsorption of Methylene Blue and Nylolan Red N-2RBL,” *Journal of Hazardous Materials*, Vol. 175, No. 1-3, 2010, pp. 779-788. [doi:10.1016/j.jhazmat.2009.10.076](https://doi.org/10.1016/j.jhazmat.2009.10.076)
- [26] V. Boonamnuayvitaya, S. Sae-ung and W. Tanthapanichakoon, “Preparation of Activated Carbons from Coffee Residue for the Adsorption of Formaldehyde,” *Separation and Purification Technology*, Vol. 42, No. 2, 2005, pp. 159-168. [doi:10.1016/j.seppur.2004.07.007](https://doi.org/10.1016/j.seppur.2004.07.007)
- [27] H. Deng, G. L. Zhang, X. L. Xu, G. H. Tai and J. L. Dai, “Optimization of Preparation of Activated Carbon from Cotton Stalk by Microwave Assisted Phosphoric Acid-Chemical Activation,” *Journal of Hazardous Materials*, Vol. 182, No. 1-3, 2010, pp. 217-224. [doi:10.1016/j.jhazmat.2010.06.018](https://doi.org/10.1016/j.jhazmat.2010.06.018)
- [28] A. E. Nembr, O. Abdelwahab, E. A. Sikaily and A. Khaled, “A Removal of Direct Blue-86 from Aqueous Solution by New Activated Carbon Developed from Orange Peel,” *Journal of Hazardous Materials*, Vol. 161, 2009, pp. 102-110.
- [29] V. K. Gupta, I. Ali, Subhas and D. Mohan, “Equilibrium Uptake and Sorption Dynamics for the Removal of a Basic Dye (Basic Red) Using Low-Cost Adsorbents,” *Journal of Colloid and Interface Science*, Vol. 265, No. 2, 2003, pp. 257-264. [doi:10.1016/S0021-9797\(03\)00467-3](https://doi.org/10.1016/S0021-9797(03)00467-3)
- [30] R. Ahmad and R. Kumar, “Adsorption Studies of Hazardous Malachite Green onto Treated Ginger Waste,” *Journal of Environmental Management*, Vol. 91, No. 4, 2010, pp. 1032-1038. [doi:10.1016/j.jenvman.2009.12.016](https://doi.org/10.1016/j.jenvman.2009.12.016)
- [31] B. H. Hameed, “Spent Tea Leaves: A Non-Conventional and Low-Cost Adsorbent for Removal of Basic Dye from Aqueous Solutions,” *Journal of Hazardous Materials*, Vol. 161, No. 2-3, 2009, pp. 753-759. [doi:10.1016/j.jhazmat.2008.04.019](https://doi.org/10.1016/j.jhazmat.2008.04.019)
- [32] I. D. Mall, V. C. Srivastava, N. K. Agarwal and I. M. Mishra, “Adsorptive Removal of Malachite Green Dye from Aqueous Solution by Bagasse Fly Ash and Activated Carbon-Kinetic Study and Equilibrium Isotherm Analyses,” *Colloids and Surface Area: Physicochemical and Engineering Aspects*, Vol. 264, No. 1-3, 2005, pp. 17-28. [doi:10.1016/j.colsurfa.2005.03.027](https://doi.org/10.1016/j.colsurfa.2005.03.027)
- [33] B. H. Hameed, D. K. Mahmoud and A. L. Ahmad, “Sorption of Basic Dye from Aqueous Solution by Pomelo (*Citrus grandis*) Peel in a Batch System,” *Colloids and Surface Area: Physicochemical and Engineering Aspects*, Vol. 316, No. 1-3, 2008, pp. 78-84. [doi:10.1016/j.colsurfa.2007.08.033](https://doi.org/10.1016/j.colsurfa.2007.08.033)
- [34] E. S. Z. E. Ashtouskhy, “*Loofa aegyptiaca* as a Novel Adsorbent for the Removal of Direct Blue Dye from Aqueous Solution,” *Journal of Environmental Management*, Vol. 90, No. 6, 2009, pp. 2755-2761. [doi:10.1016/j.jenvman.2009.03.005](https://doi.org/10.1016/j.jenvman.2009.03.005)
- [35] I. Langmuir, *Journal of the American Chemical Society*, Vol. 40, 1918, p. 1361.
- [36] M. Dogan, M. Alkan and Y. Onganer, “Adsorption of Methylene Blue from Aqueous Solution onto Perlite,” *Water, Air and Soil Pollution*, Vol. 120, No. 3-4, 2000, pp. 229-249. [doi:10.1023/A:1005297724304](https://doi.org/10.1023/A:1005297724304)
- [37] I. Langmuir, “The Constitution and Fundamental Properties of Solids and Liquids,” *Journal of the American Chemical Society*, Vol. 38, No. 11, 1916, pp. 2221-2295. [doi:10.1021/ja02268a002](https://doi.org/10.1021/ja02268a002)
- [38] D. G. Kinniburgh, “General Purpose Adsorption Isotherms,” *Environmental Science & Technology*, Vol. 20, No. 9, 1986, pp. 895-904. [doi:10.1021/es00151a008](https://doi.org/10.1021/es00151a008)
- [39] E. Longhinotti, F. Pozza, L. Furlan, M. D. N. D. Sanchez, M. Klug, M. C. M. Laranjeira and V. T. Favere, “Adsorption of Anionic Dyes on the Biopolymer Chitin,” *Journal of the Brazilian Chemical Society*, Vol. 9, No. 5, 1998, pp. 435-440. [doi:10.1590/S0103-50531998000500005](https://doi.org/10.1590/S0103-50531998000500005)
- [40] H. Freundlich, “User Die Adsorption in Losungen (Ad-

- sorption in Solution),” *The Journal of Physical Chemistry*, Vol. 57, 1906, pp. 384-470.
- [41] B. Acemioglu, “Adsorption of Congo Red from Aqueous Solution onto Calcium-Rich Fly Ash,” *Journal of Colloid and Interface Science*, Vol. 274, No. 2, 2004, pp. 371-379. [doi:10.1016/j.jcis.2004.03.019](https://doi.org/10.1016/j.jcis.2004.03.019)
- [42] J. P. Hobson, “Physical Adsorption Isotherms Extending from Ultrahigh Vacuum to Vapor Pressure,” *The Journal of Physical Chemistry*, Vol. 73, No. 8, 1969, pp. 2720-2727. [doi:10.1021/j100842a045](https://doi.org/10.1021/j100842a045)
- [43] M. J. Temkin and V. Pyzhev, “Recent Modifications to Langmuir Isotherms,” *Acta Physiochim, URSS* 12, 1940, pp. 217-222.
- [44] K. Y. Foo and B. H. Hameed, “Insights into the Modeling of Adsorption Isotherm Systems,” *Chemical Engineering Journal*, Vol.156, No. 1, 2010, pp. 2-10. [doi:10.1016/j.cej.2009.09.013](https://doi.org/10.1016/j.cej.2009.09.013)
- [45] A. C. Duran and I. Flores, “Evaluation of Lead (II) Immobilization by a Vermicompost Using Adsorption Isotherms and IR Spectroscopy,” *Bioresource Technology*, Vol. 100, No. 4, 2009, pp. 1691-1694. [doi:10.1016/j.biortech.2008.09.013](https://doi.org/10.1016/j.biortech.2008.09.013)
- [46] G. Crini, H. N. Peindy, F. Gimbert and C. Robert, “Removal of C.I. Basic Green 4 (Malachite Green) from Aqueous Solutions by Adsorption Using Cyclodextrin-Based Adsorbent: Kinetic and Equilibrium Studies,” *Separation and Purification Technology*, Vol. 53, No. 1, 2007, pp. 97-110. [doi:10.1016/j.seppur.2006.06.018](https://doi.org/10.1016/j.seppur.2006.06.018)
- [47] M. Ozacar and I. A. Sengil, “A Kinetic Study of Metal Complex Dye Sorption onto Pine Sawdust,” *Process Biochemistry*, Vol. 40, No. 2, 2005, pp. 565-572. [doi:10.1016/j.procbio.2004.01.032](https://doi.org/10.1016/j.procbio.2004.01.032)
- [48] G. H. Sonawane and V. S. Shrivastava, “Kinetics of Decolourization of Malachite Green from Aqueous Medium by Maize Cob (*Zea mays*): An Agricultural Solid Waste,” *Desalination*, Vol. 247, No. 1-3, 2009, pp. 430-441. [doi:10.1016/j.desal.2009.01.006](https://doi.org/10.1016/j.desal.2009.01.006)
- [49] W. J. Weber and J. C. Morris, “Kinetics of Adsorption on Carbon from Solution,” *Journal of Sanitary Engineering Division of the American Society of Civil Engineering*, Vol. 89, 1963, pp. 31-59.
- [50] Y. S. Ho, “Removal of Copper Ions from Aqueous Solution by Tree Fern,” *Water Research*, Vol. 37, No. 10, 2003, pp. 2323-2330. [doi:10.1016/S0043-1354\(03\)00002-2](https://doi.org/10.1016/S0043-1354(03)00002-2)
- [51] S. H. Chen, J. Zhang, C. G. Zhang, Q. Y. Yue, Y. Li and C. Li, “Equilibrium and Kinetic Studies of Methyl Orange and Methyl Violet Adsorption on Activated Carbon Derived from *Phragmites australis*,” *Desalination*, Vol. 252, No. 1-3, 2010, pp. 149-156. [doi:10.1016/j.desal.2009.10.010](https://doi.org/10.1016/j.desal.2009.10.010)